

**U.S. DEPARTMENT OF COMMERCE  
National Technical Information Service**

**AD-A030 952**

# **An Experimental Study of Moisture Migration in Concrete**

**Army Engineer Waterways Experiment Station Vicksburg Miss**

**Sep 70**

## BEST SELLERS

FROM NATIONAL TECHNICAL INFORMATION SERVICE

**NTIS**

- Product Liability Insurance: Assessment of Related Problems and Issues. Staff Study**  
PB-252 204/PAT 181 p PC\$9.50/MF\$3.00

**Evaluation of Home Solar Heating System**  
UCRL-51 711/PAT 154 p PC\$6.75/MF\$3.00

**Developing Noise Exposure Contours for General Aviation Airports**  
ADA-023 429/PAT 205 p PC\$7.75/MF\$3.00

**Cooling Tower Environment, 1974. Proceedings of a Symposium Held at the University of Maryland Adult Education Center on Mar. 4-6, 1974**  
CONF-74 0302/PAT 648 p PC\$13.60/MF\$3.00

**Biological Services Program. Fiscal Year 1975**  
PB-251 738/PAT 52 p PC\$4.50/MF\$3.00

**An Atlas of Radiation Histopathology**  
TID-26-676/PAT 234 p PC\$7.60/MF\$3.00

**Federal Funding of Civilian Research and Development. Vol. 1. Summary**  
PB-251 266/PAT 61 p PC\$4.50/MF\$3.00

**Federal Funding of Civilian Research and Development. Vol. 2. Case Studies**  
PB-251 683/PAT 336 p PC\$10.00/MF\$3.00

**Handbook on Aerosols**  
TID-26-806/PAT 141 p PC\$6.00/MF\$3.00

**for the Assessment of Ocean Outfalls**  
ADA-023 514/PAT 34 p PC\$4.00/MF\$3.00

**Guidelines for Documentation of Computer Programs and Automated Data Systems**  
PB-250 867/PAT 54 p PC\$4.50/MF\$3.00

**NOx Abatement for Stationary Sources in Japan**  
PB-250 586/PAT 116 p PC\$5.50/MF\$3.00

**U.S. Coal Resources and Reserves**  
PB-252 752/PAT 16 p PC\$3.50/MF\$3.00

**Structured Programming Series. Vol. XI. Estimating Software Project Resource Requirements**  
ADA-016 416/PAT 70 p PC\$4.50/MF\$3.00

**Assessment of a Single Family Residence Solar Heating System in a Suburban Development Setting**  
PB-246 141/PAT 244 p PC\$8.00/MF\$3.00

**Technical and Economic Study of an Underground Mining, Rubblization, and in Situ Retorting System for Deep Oil Shale Deposits. Phase I Report**  
PB-249 344/PAT 223 p PC\$7.75/MF\$3.00

**A Preliminary Forecast of Energy Consumption Through 1985**  
PB-251 445/PAT 69 p PC\$4.50/MF\$3.00

# **HOW TO ORDER**

When you indicate the method of payment, please note if a purchase order is not accompanied by payment, you will be billed an addition \$5.00 ship and bill charge. And please include the card expiration date when using American Express.

Normal delivery time takes three to five weeks. It is vital that you order by number

or your order will be manually filled, insuring a delay. You can opt for airmail delivery for a \$2.00 charge per item. Just check the Airmail Service box. If you're really pressed for time, call the NTIS Rush Order Service (703) 557-4700. For a \$10.00 charge per item, your order will be airmailed within 48 hours. Or, you can pick up your order in the Washington Information Center & Bookstore or at our Springfield Operations Center within 24 hours for a \$6.00 per item charge.

You may also place your order by telephone or TELEX. The order desk number is (703) 557-4650 and the TELEX number is 89-9403.

Whenever a foreign sales price is NOT specified in the listings, all foreign buyers must add the following charges to each order: \$2.50 for each paper copy; \$1.50 for each microfiche; and \$10.00 for each Published Search.

Thank you for your interest in NTIS. We appreciate your order.

**METHOD OF PAYMENT**

- Charge my NTIS deposit account no. \_\_\_\_\_
  - Purchase order no. \_\_\_\_\_
  - Check enclosed for \$ \_\_\_\_\_
  - Charge to my American Express Card account number \_\_\_\_\_

A horizontal row of 12 empty rectangular boxes, likely for students to write their answers in a worksheet.

**Card expiration date:** \_\_\_\_\_

**Signature**

- Airmail Services requested

**Clip and mail to**



National Technical Information Service  
U.S. DEPARTMENT OF COMMERCE  
Springfield, Va. 22161  
(703) 557-4650 TELEX 89-9405

(703) 557-4650 TELEX 39-9405

**NAME** \_\_\_\_\_

**ADDRESS.** \_\_\_\_\_

CITY, STATE, ZIP \_\_\_\_\_

Item Number	Quantity		Unit Price*	Total Price
	Paper Copy (PC)	Microfiche (MF)		

All Prices Subject to Change

1176

**Sub Total**  
**Additional Charge**  
**Enter Grand Total**



1

MISCELLANEOUS PAPER C-70-15

AN EXPERIMENTAL STUDY OF MOISTURE  
MIGRATION IN CONCRETE

by

J. E. McDonald



RESEARCH CENTER LIBRARY  
U.S. ARMY ENGINEER WATERWAYS EXPERIMENT STATION  
VICKSBURG, MISSISSIPPI

D D C  
REPROD BY  
OCT 19 1976

September 1970

Sponsored by U. S. Atomic Energy Commission

Conducted by U. S. Army Engineer Waterways Experiment Station, Vicksburg, Mississippi

REPRODUCED BY  
NATIONAL TECHNICAL  
INFORMATION SERVICE

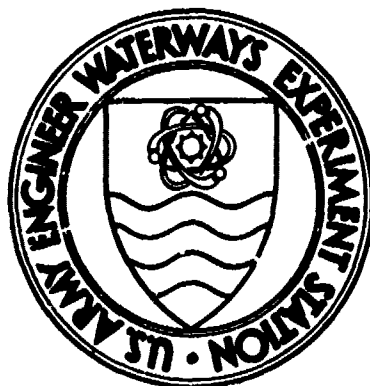
U. S. DEPARTMENT OF COMMERCE  
SPRINGFIELD, VA. 22161

This document has been

distribution is unlimited

**Destroy this report when it 's no longer needed.  
Do not return it to the originator.**

**The findings in this report are not to be construed as an official  
Department of the Army position unless so designated  
by other authorized documents.**



MISCELLANEOUS PAPER C-70-15

## AN EXPERIMENTAL STUDY OF MOISTURE MIGRATION IN CONCRETE

by

J. E. McDonald



September 1970

D D C  
DRAFTED BY  
OCT 19 1976  
RELEASER  
D

Sponsored by U. S. Atomic Energy Commission

Conducted by U. S. Army Engineer Waterways Experiment Station, Vicksburg, Mississippi

ARMY-NRC MICROFILM, 1960.

This document has been approved for public release and sale; its distribution is unlimited

### Foreword

This paper was prepared for the American Concrete Institute (ACI) Seminar on Concrete for Nuclear Reactors, held at Berlin, Germany, on 4-11 October 1970. The manuscript was reviewed and cleared for publication by the Oak Ridge National Laboratory and the Office, Chief of Engineers, U. S. Army.

The study which provided the information and data discussed herein is being conducted by the U. S. Army Engineer Waterways Experiment Station (WES), Vicksburg, Miss., under the sponsorship of the U. S. Atomic Energy Commission. This continuing investigation was initiated in 1966. Staff members actively involved in the investigation include Mr. Bryant Mather, Chief of the WES Concrete Division, Mr. J. M. Polatty, Chief of the Engineering Mechanics Branch, Dr. H. G. Geymayer, former Chief of the Structures Section, and Dr. J. C. Chakrabarti. Mr. James E. McDonald, current project engineer for this investigation, prepared this paper.

Directors of the WES during the conduct of this investigation and preparation of this paper were COL John R. Oswalt, Jr., CE; COL Levi A. Brown, CE; and COL Ernest D. Peiotto, CE. Technical Directors were Mr. J. B. Tiffany and Mr. F. R. Brown.

## Contents

	<u>Page</u>
Foreword . . . . .	iii
Summary. . . . .	vii
Background . . . . .	1
Purpose and Scope of Study . . . . .	1
Instrumentation. . . . .	2
Test Specimen. . . . .	3
Effects of Concrete Hydration. . . . .	4
Temperature. . . . .	4
Moisture . . . . .	5
Strains. . . . .	6
Effects of a Temperature Gradient. . . . .	6
Temperature. . . . .	7
Moisture . . . . .	7
Strains. . . . .	8
Discussion . . . . .	8
Figures 1-24	

### Summary

In an effort to obtain information regarding the nature of moisture movement and rate of moisture loss in a prestressed concrete reactor vessel (PCRV), an experimental study of moisture migration in a pie-shaped specimen representing the flow path through a cylindrical wall of a PCRV was initiated. After casting of the test specimen, temperature distribution, shrinkage, and moisture distribution were monitored for approximately 17 months. After this initial testing, a temperature gradient of 80 F (44 C) was applied to the specimen, and the above-mentioned measurements are being continued for an additional test period of one year. Based on the results obtained to date, it appears that there have been no significant changes in the specimen's moisture content.

## AN EXPERIMENTAL STUDY OF MOISTURE MIGRATION IN CONCRETE

### Background

1. The use of prestressed concrete in construction of nuclear reactor pressure vessels is a departure from usual civil engineering practice, and, as would be expected, many unusual problems arise in the design and construction of such a vessel. In spite of the tremendous amount of research on the properties of concrete, information regarding certain properties of concrete under particular conditions is often insufficient. This appears to be especially true in the case of the use of prestressed concrete for reactor pressure vessels. One of the most important aspects in the design and safety evaluation of a prestressed concrete reactor vessel (PCRV) is the time-dependent deformation behavior of concrete in the presence of varying temperature, moisture, and loading conditions. Consequently, a basic research program formulated and directed by the Oak Ridge National Laboratory for the purpose of developing and improving the technology of PCRV's in the United States included a sizable effort directed toward investigating the time-dependent deformation behavior of concrete under conditions existing in a PCRV. One of the projects included in this effort was a test of the moisture distribution in a PCRV wall performed at the U. S. Army Engineer Waterways Experiment Station and reported herein.

### Purpose and Scope of Study

2. Information regarding the nature of moisture movement and rate of moisture loss in a concrete pressure vessel wall subjected to a temperature gradient is of interest in view of the influence of these parameters on the properties of concrete. In an effort to evaluate these effects, an experimental study of moisture migration in a pie-shaped concrete specimen (fig. 1) representing the flow path or channel through a cylindrical wall of a PCRV was initiated.

3. The test specimen selected was 9 ft (2.74 m) in length with

cross-sectional dimensions of 2 by 2 ft (0.61 by 0.61 m) on one end and 2 ft by 2 ft 8 in. (0.61 by 0.81 m) on the other end. The specimen was sealed against moisture loss on the small end (interior) and along the lateral surfaces, and exposed to the atmosphere on the other end (exterior). In addition, the lateral surfaces were heated and insulated to simulate conditions in a PCRV where uniaxial moisture and heat flow prevail.

4. After casting of the test specimen, the temperature distribution, shrinkage, and moisture distribution were monitored for approximately 17 months. After this initial testing, a temperature gradient of 80 F (44 C) was applied to the specimen and the above-mentioned measurements are being continued for an additional test period of one year.

#### Instrumentation

5. Carlson strain meters were embedded as shown in fig. 2 to determine the variation in concrete strain and temperature along the center line of the specimen. Iron-constantan thermocouples were embedded at five different depths at each of three different sections as shown in fig. 3 to determine temperature profiles at sections near each end and the center of the specimen. Removable plugs in the casting form and insulation along the top surface of the specimen (fig. 4) allowed the use of a surface back-scatter nuclear gage to determine moisture content of the concrete at various stations along the specimen. Open-wire-line (OWL) probes were embedded along a lateral surface of the specimen, as shown in fig. 5, to measure relative dielectric constants which appear to be sensitive measurement parameters for moisture content. Wells for Monfore probes were provided along the same surface (fig. 6) for relative humidity measurements.

6. In an effort to approach the adiabatic boundary conditions essential to study the effect of hydration heat dissipation and to ensure uniaxial heat and moisture flow, lateral surfaces of the specimen were heated and insulated. Heating was accomplished with eight independent resistance wire heating elements wrapped around the specimen. These elements were actuated by a series of thermistors embedded at the center and boundary region at each cross section indicating temperature differentials between

the core and the boundary of the specimen. When, and in whatever section, a temperature differential of 1 F (0.6 C) was indicated, a relay automatically actuated the pertinent heating element until a uniform temperature distribution was restored.

#### Test Specimen

7. The casting form for the moisture migration specimen with instrumentation, insulation, and moisture barrier in place is shown in fig. 7 immediately prior to casting. A concrete mixture proportioned with 3/4-in. (1.9-cm) maximum size crushed limestone aggregate to have a slump of  $2 \pm 1/2$  in. ( $5.1 \pm 1.3$  cm) and a compressive strength of 6000 psi ( $422 \text{ kg/cm}^2$ ) at 28 days was used in casting the specimen. Mixture proportions were as follows:

Material	Solid Volume		Saturated Surface Dry Batch Weight	
	ft <sup>3</sup>	(m <sup>3</sup> )	lb	(kg)
Type II cement	3.473	(0.0983)	681.5	(309.1)
Fine aggregate	8.305	(0.2352)	1381.5	(626.6)
Coarse aggregate	10.569	(0.2993)	1784.4	(809.4)
Water	4.653	(0.1318)	289.86	(131.48)

The foregoing quantities are theoretical proportions for 1 yd<sup>3</sup> (0.7645 m<sup>3</sup>) of concrete having no air content and aggregate without absorption. The aggregates were batched dry and 26.6 lb (12.1 kg) of additional water was added to the batch to satisfy the absorption of the aggregates. Thus, a theoretical cubic yard of concrete, air free, included 316.46 lb (143.54 kg) of water or 11.72 lb/ft<sup>3</sup> (187.7 kg/m<sup>3</sup>). The air content of the concrete was about 3 percent. Therefore a cubic foot of actual volume of freshly mixed concrete of this mixture is calculated to consist of the following:

Material	Volume		Weight	
	ft <sup>3</sup>	(m <sup>3</sup> )	lb	(kg)
Air	0.030	(0.00085)	--	--
Cement	0.125	(0.00354)	24.46	(11.09)
Water (mixing)	0.167	(0.00473)	10.40	(4.72)

(Continued)

	Volume		Weight	
	ft <sup>3</sup>	(m <sup>3</sup> )	lb	(kg)
Water (absorption)*	0.015	(0.00042)	0.96	(0.44)
Fine aggregate*	0.298	(0.00844)	49.58	(22.49)
Coarse aggregate*	0.380	(0.01076)	64.03	(29.04)
Total	1.000	(0.02832)	148.47	(67.34)

\* Water added to satisfy aggregate absorption not included in total; aggregate volume and weight include absorbed water.

8. Upon completion of casting, the top was closed and moisture-sealed to the remainder of the form. At seven days age, the plywood forms were removed from the ends of the specimen, exposing the open end to the controlled atmosphere of  $70 \pm 3^{\circ}\text{F}$  ( $21 \pm 1.7^{\circ}\text{C}$ ) temperature and  $50 \pm 1$  percent relative humidity.

#### Effects of Concrete Hydration

##### Temperature

9. Temperature in the freshly placed concrete rose at a continuously increasing rate during the first 10 hours after casting (fig. 8). During the next 15 hours, the temperature rose, but at a continuously decelerating rate, and peaked at all stations between 29 and 98 hours after placing of the concrete. Inner stations recorded higher peak temperatures and a longer rise than the stations nearer the ends, though all stations, with the exception of 4 and 5 (Carlson gages), recorded about 90 percent of the respective maximum temperature rise within about 30 hours after casting. This behavior indicates that after a relatively short initial period (about 30 hours) the rate of heat dissipation (heat flow toward the two cool faces of the specimen) was nearly the same as the rate of heat release resulting from cement hydration. Within 100 hours, more heat was being dissipated than was being released in all portions of the specimen. Due to the relatively fast flow of heat toward the two cool end faces of the specimen, temperatures in the concrete never approached the value that would have been expected under adiabatic conditions.

10. The highest temperature recorded, near the midsection of the specimen, was 168 F (76 C), a rise of 93 F (52 C). The lowest peak recorded was 127 F (53 C), a rise of 56 F (31 C), occurring at the gage nearest the open end. After reaching the peak values, temperatures started falling at a very gradual rate (fig. 9), stabilizing near room temperature about 60 days after casting.

11. Iron-constantan thermocouples were used to monitor temperatures at five different depths in each of three sections, two at the two ends and one at the center. Temperatures monitored by thermocouples 1-10, 12, and 14 were recorded on a strip-chart recorder; thermocouples 11, 13, and 15 were read manually. Temperatures were fairly constant at different depths within a section (fig. 10), but varied between sections, the highest temperature being at the midsection and the lowest near the open end.

#### Moisture

12. Moisture in the concrete, as indicated by the nuclear surface moisture gage, was fairly constant in all the sections except the two ends, particularly the open end. The gage indicated a fairly uniform decrease in water content of the concrete at station 10 (nearest the open end) during the first week after casting. Apparent decreases of approximately  $1 \text{ lb/ft}^3$  ( $16 \text{ kg/m}^3$ ) at each end coincided with removal of the plywood forms at each end seven days after casting. At this time, the water content in each end tended to level out between  $11$  and  $12 \text{ lb/ft}^3$  ( $176$  and  $192 \text{ kg/m}^3$ ). The maximum moisture content appeared to be approximately  $13.5 \text{ lb/ft}^3$  ( $216 \text{ kg/m}^3$ ) at the interior sections (fig. 11).

13. The maximum indicated water content of  $13.5 \text{ lb/ft}^3$  ( $216 \text{ kg/m}^3$ ) is somewhat higher than the theoretical water content of  $11.36 \text{ lb/ft}^3$  ( $182 \text{ kg/m}^3$ ) computed previously for this mixture. It is possible that moisture collecting on top of the specimen immediately under the moisture barrier as a result of the concrete bleeding would cause the surface backscatter gage, which penetrates only the top few inches and reflects the moisture content of a parabolic section (the greater area being on the surface), to indicate moisture content higher than that actually present near the center of the specimen. In addition, the tops of concrete surfaces normally have an increased amount of mortar, and consequently a higher moisture content.

14. The OWL probes indicated variations in relative dielectric constant with time in each of the sections. Data from typical probes are shown in fig. 12. It was apparent that the null frequencies and, consequently, the relative dielectric constant were affected not only by the moisture content in the concrete but also by the temperature and maturity of the concrete. The influences of these two parameters are presently being evaluated in a separate study.

15. These probes appeared to function properly for approximately 12 months after casting. At that time, readings from several gages became quite erratic, and in some cases, it was extremely difficult to obtain null frequencies which would yield realistic moisture contents. Developers of this gage indicate that the gage may have corroded even though it was silver-plated prior to embedment.

16. The Monfore relative humidity probes furnished limited useful information about the moisture content in the concrete during this phase because the temperature of the concrete during hydration exceeded the operational range of this probe. As the temperature dropped to within the probe limits, all wells indicated relative humidities close to 100 percent, as expected. As the concrete temperature approached room temperature, the Monfore probes stabilized within the range  $96 \pm 2$  percent relative humidity.

#### Strains

17. Variations of total concrete strain with time are indicated in fig. 13. The maximum value of indicated strain was about 500 microstrains at an inner section, while the minimum peaks recorded were about 300 microstrains near the ends. After reaching the peak values, strains at each station began to decrease at a gradual rate (fig. 14), stabilizing at values less than 100 microstrains expansion about 60 days after casting. In an effort to determine any nonthermal strains present in the specimen, total strains were corrected for thermal effects, assuming a linear coefficient of thermal expansion of  $\frac{5.0}{^{\circ}\text{F}} \times 10^{-6}$   $\left(\frac{9.0}{^{\circ}\text{C}} \times 10^{-6}\right)$ . Results for typical gages are shown in fig. 15.

#### Effects of a Temperature Gradient

18. Strain, temperature, and moisture in the concrete were in

essentially steady states prior to application of the temperature gradient of 80 F (44 C) to the specimen approximately 17 months after casting. A series of heat lamps (fig. 16) is being used to maintain the required temperature on the simulated interior vessel face. Since application of the temperature gradient, data regarding changes in temperature, moisture, and strain have been obtained regularly and are discussed briefly in the following paragraphs.

#### Temperature

19. The variation in concrete temperature along the specimen's center line is being determined by means of Carlson strain meters embedded as previously shown (fig. 2). As a result of the temperature gradient, concrete temperatures within the specimen continue to increase but at a decreasing rate as shown in fig. 17. As expected, temperature increases in the early stages after application of heat were confined to that half of the specimen nearer the heat. After approximately one week, relatively uniform increases in temperature were noted throughout the specimen. Temperature variations with time for typical individual gages are shown in fig. 18. Latest temperature measurements (127 days after heating) are essentially the same as those at 43 days.

20. Temperatures monitored by thermocouples at five different depths in each of three sections were fairly constant at different depths within a section but varied between sections, the highest temperature being near the heated end and the lowest near the open end. A temperature profile (fig. 19) of the section nearest the heat indicates that the temperature differential between the interior and exterior of the specimen is within 1 F (0.6 C) at present.

#### Moisture

21. A surface backscatter nuclear gage was used to determine concrete moisture contents at various stations along the top surface of the specimen (fig. 14). Representative plots of moisture content determined in this manner (fig. 20) indicate no significant changes in the specimen's moisture content since application of the temperature gradient.

22. As previously noted, the CMI probe is influenced by variations in temperature; therefore, application of the temperature gradient resulted

in apparent increases in the relative dielectric constant as shown in fig. 21. However, as the temperature tended to stabilize, output from the O.W.L probes attained an essentially steady state, indicating no change in the specimen's moisture content.

23. Prior to application of heat, the Monfore relative humidity probes indicated that the relative humidities in each well were in an essentially steady state at approximately 96 percent. Upon application of heat, the indicated relative humidity in those wells nearest the heat increased rapidly to 100 percent, and within 21 days, all wells, with the exception of the three nearest the open end, were at 100 percent relative humidity. The three wells nearest the open end continue to indicate relative humidities ranging from 90 to 97 percent.

#### Strains

24. Variations in concrete strain along the specimen's center line as a result of applying a temperature gradient are presented in fig. 22. The highest indicated strain is about 340 microstrains at the station nearest the heat. From this maximum, indicated strains decrease in a generally linear manner to less than 25 microstrains near the open end. Strain variations with time at typical stations are shown in fig. 23. As expected, these curves are of the same general shape as those of temperature versus time. When the total strains are corrected for thermal expansion of the specimen (fig. 24), it is obvious that the specimen remains in an essentially steady-state strain condition with no significant changes as a result of applying the temperature gradient.

#### Discussion

25. The fairly uniform temperatures at different depths within a section and the relatively fast flow of heat toward the two cool faces of the specimen during cement hydration indicate that the boundary conditions are sufficient to simulate the flow path through a cylindrical wall of a PCW where uniaxial moisture and heat flow prevail.

26. Since application of the temperature gradient, data regarding changes in temperature, moisture, and strain have been obtained regularly

for approximately one-third the anticipated one-year test period. Based on the results obtained to date, it appears that there have been no significant changes in the specimen's moisture content since application of the temperature gradient. Consequently, it may be tentatively assumed that the moisture movement and rate of moisture loss in a PCRV wall subjected to a temperature gradient are such that these parameters should not affect the properties of the concrete. However, it is emphasized that this test is incomplete at present, and the nature of moisture movement and rate of moisture loss could change drastically as the experiment continues.

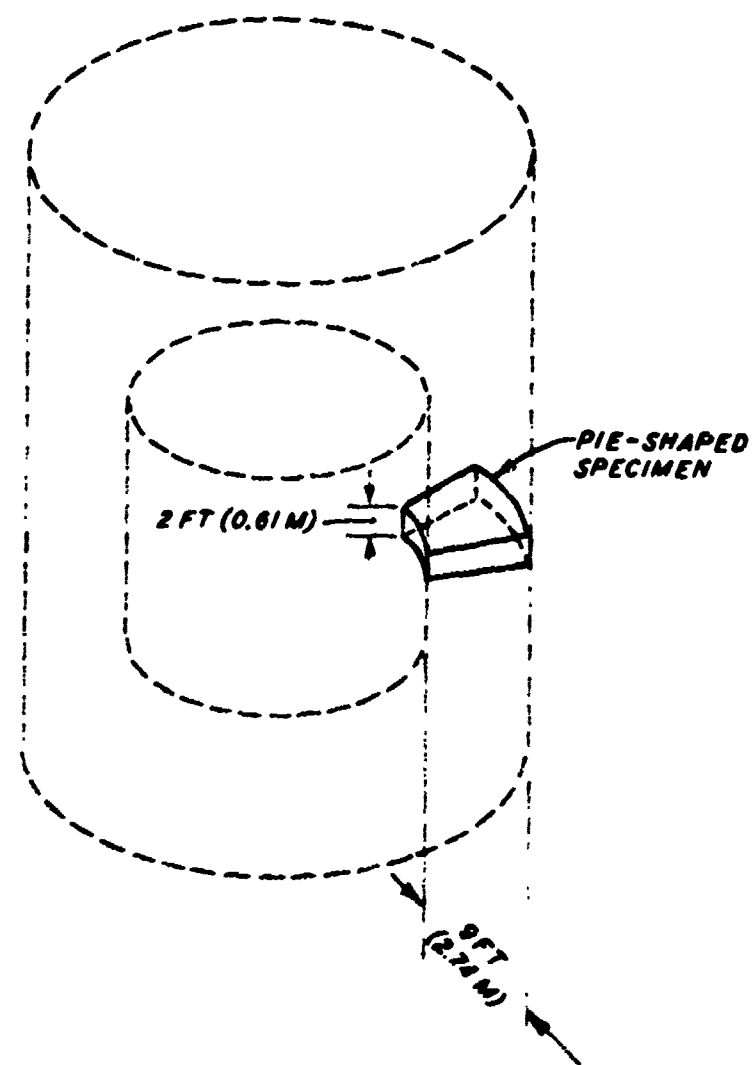


Fig. 1. Simulated location of specimen in vessel

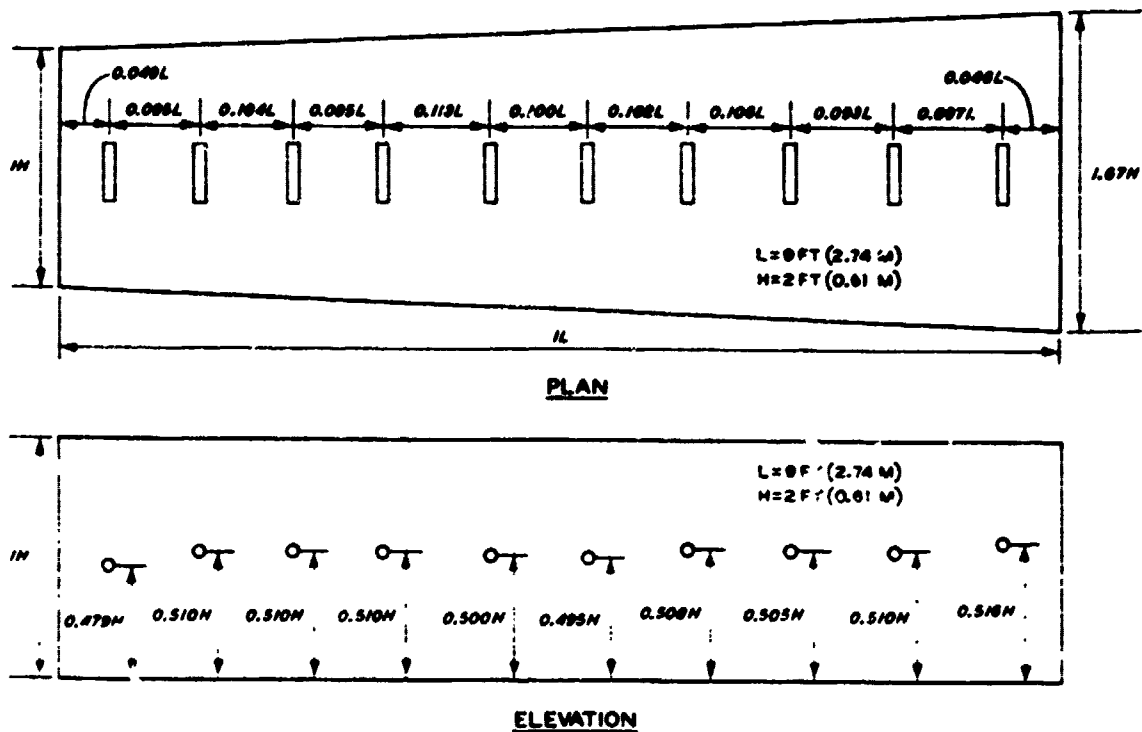


Fig. 2. Carlson strain meter locations

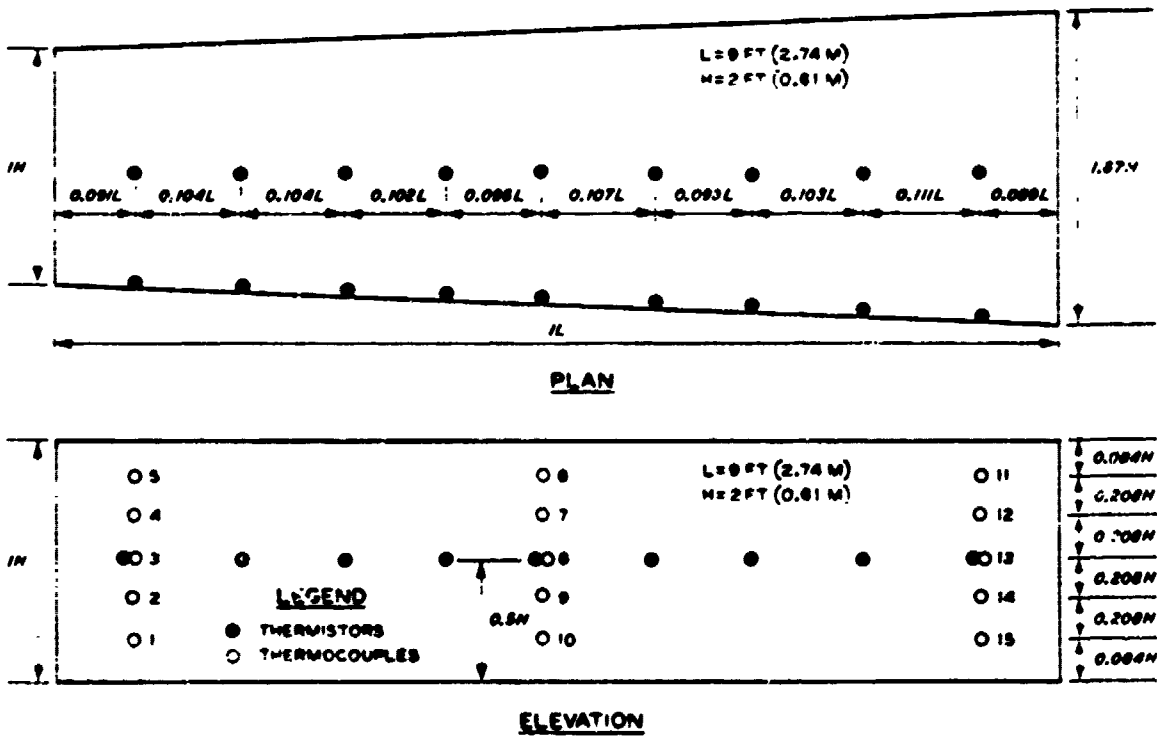


Fig. 3. Thermocouple and thermistor locations

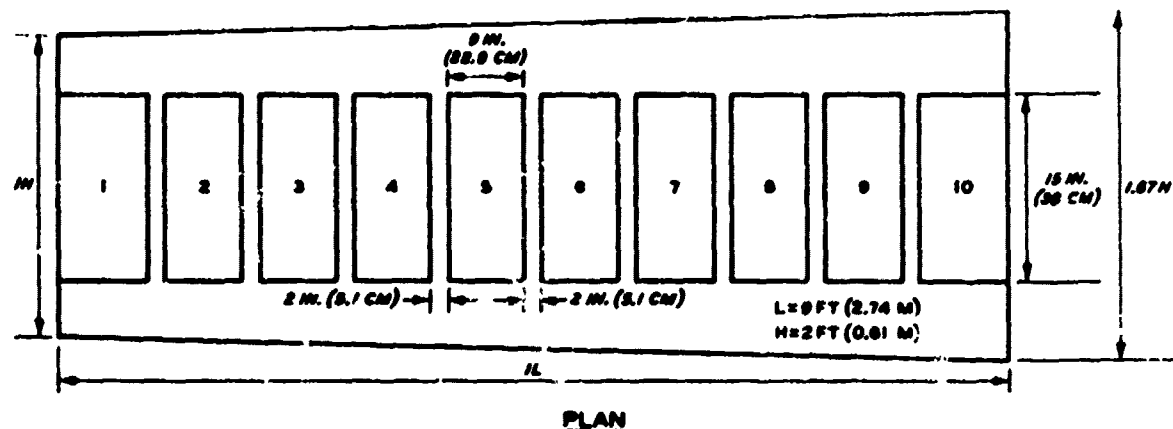


Fig. 4. Nuclear moisture gage stations

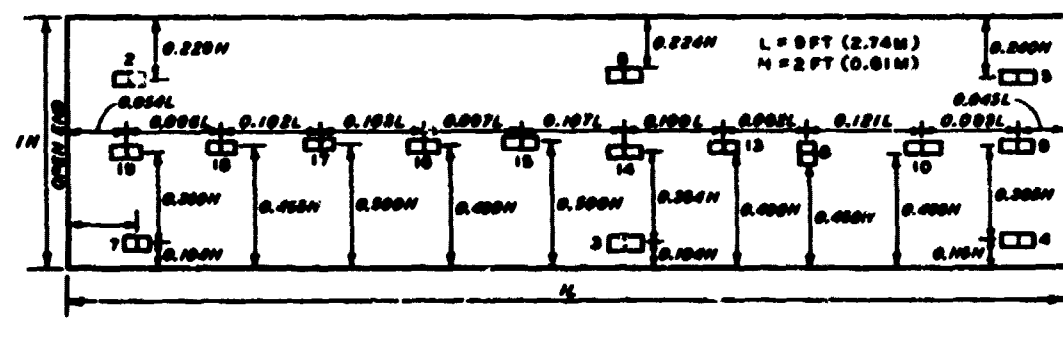


Fig. 5. Position of OWL gages

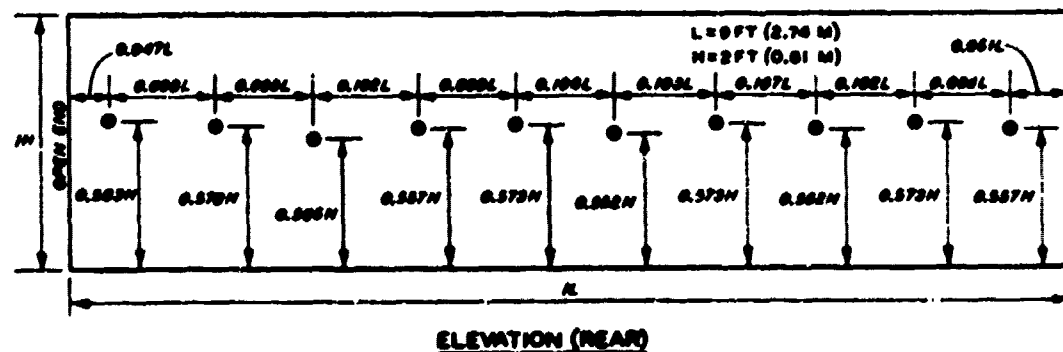


Fig. 6. Monfore gage locations

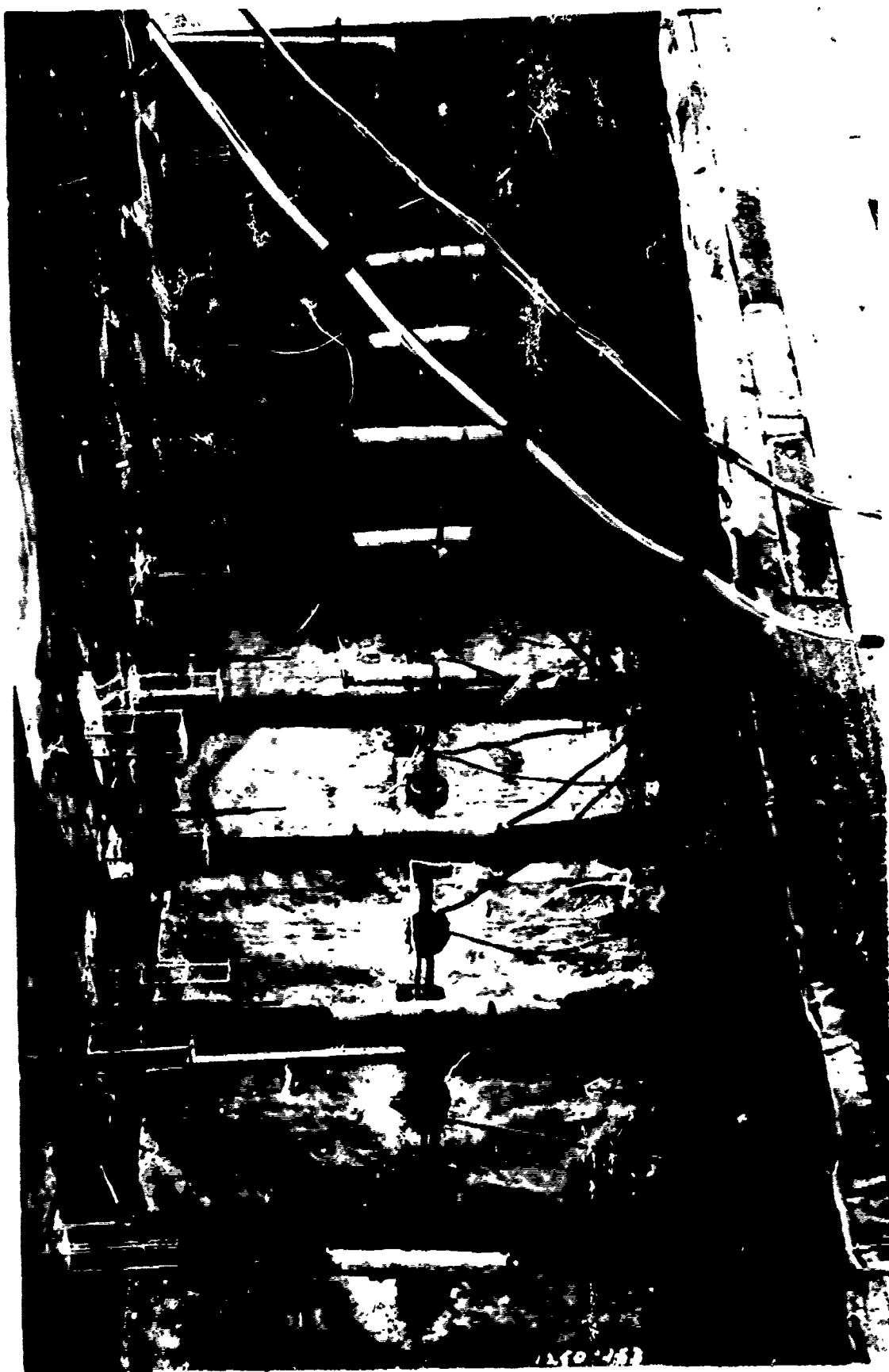


Fig. 7. Embedded instrumentation for moisture migration studies - view from closed end

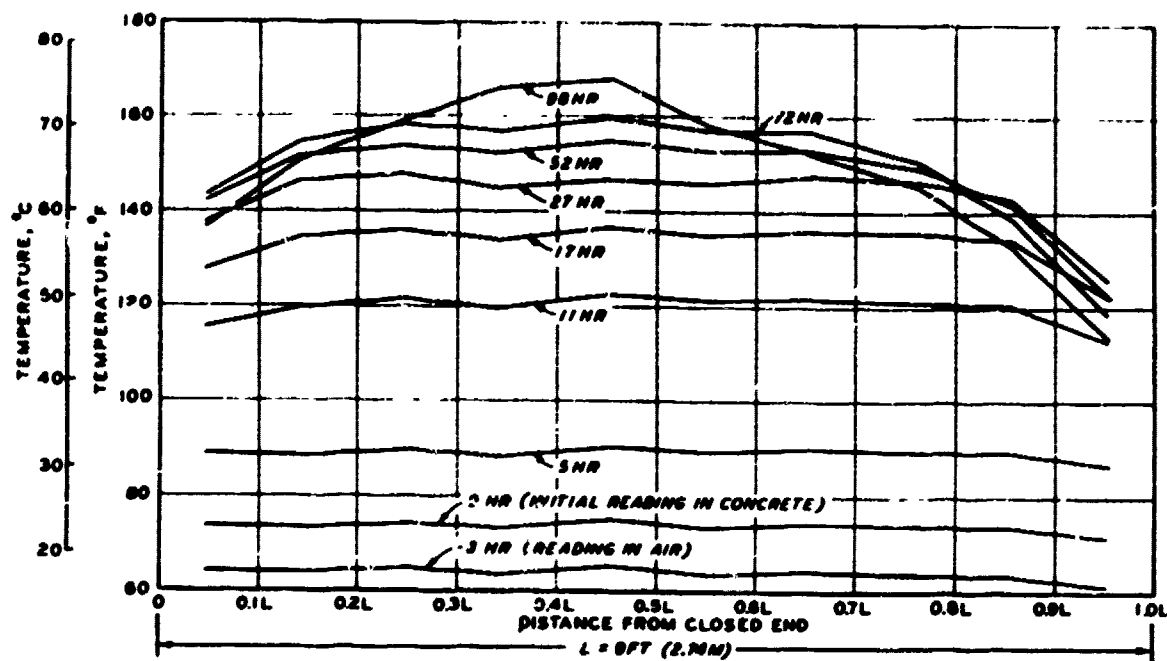


Fig. 8. Temperature rise

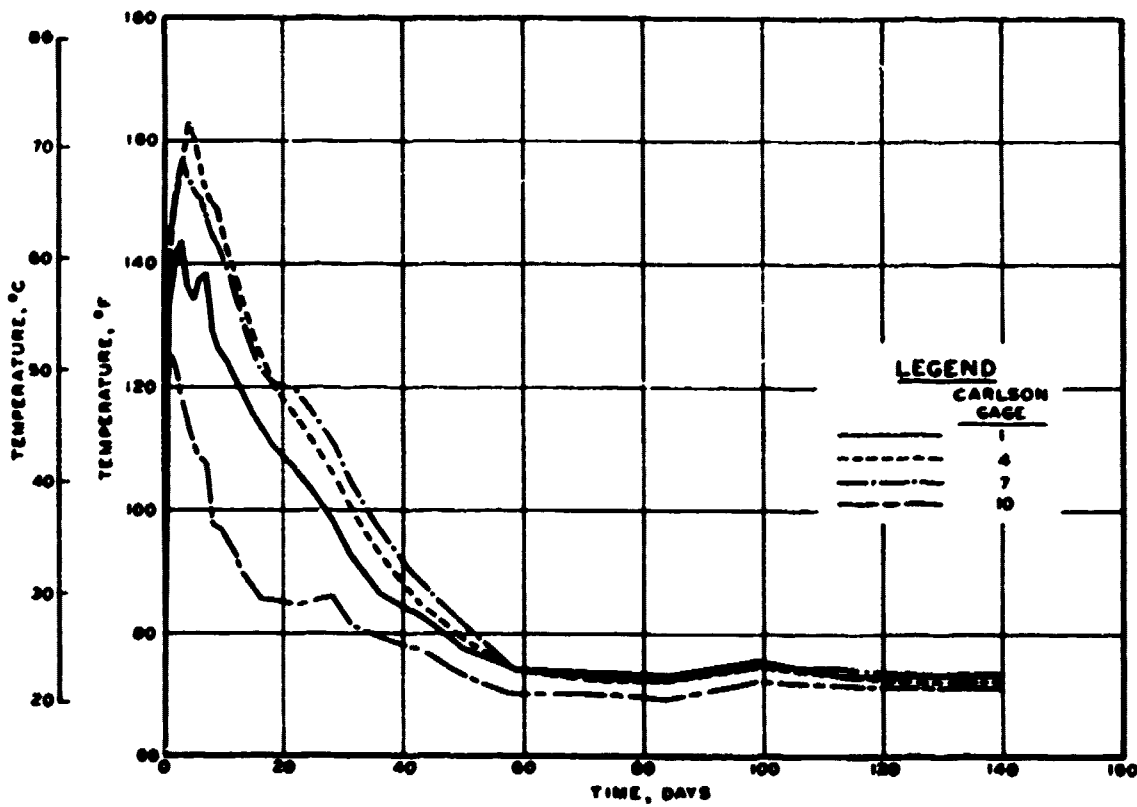


Fig. 9. Temperature versus time

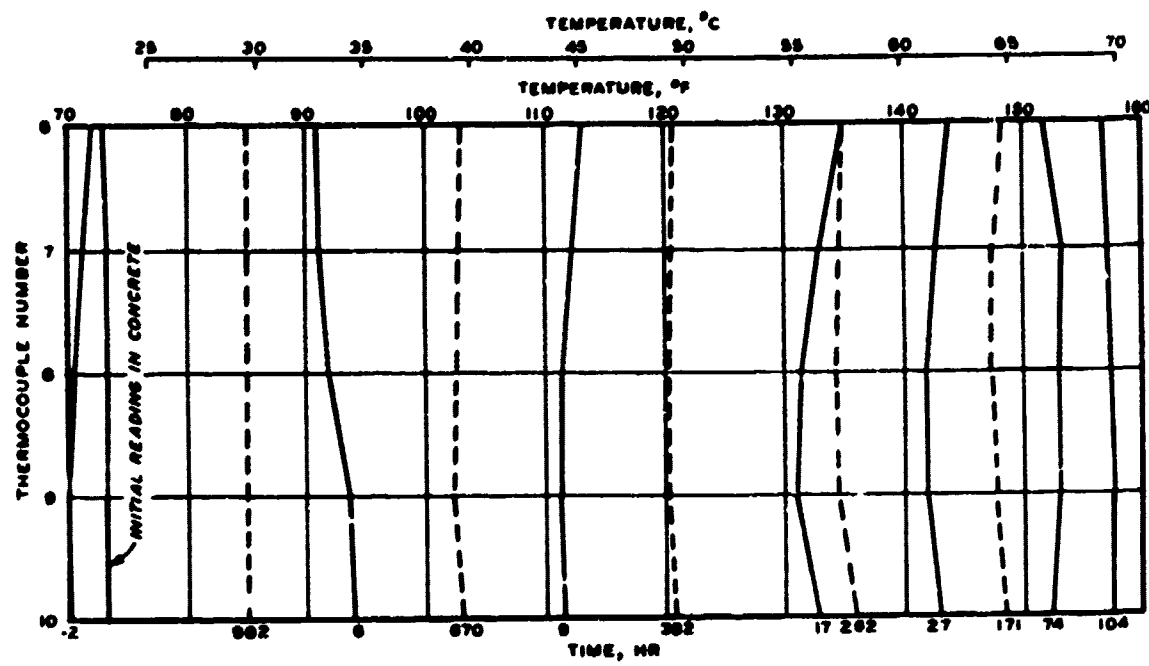


Fig. 10. Temperature profile

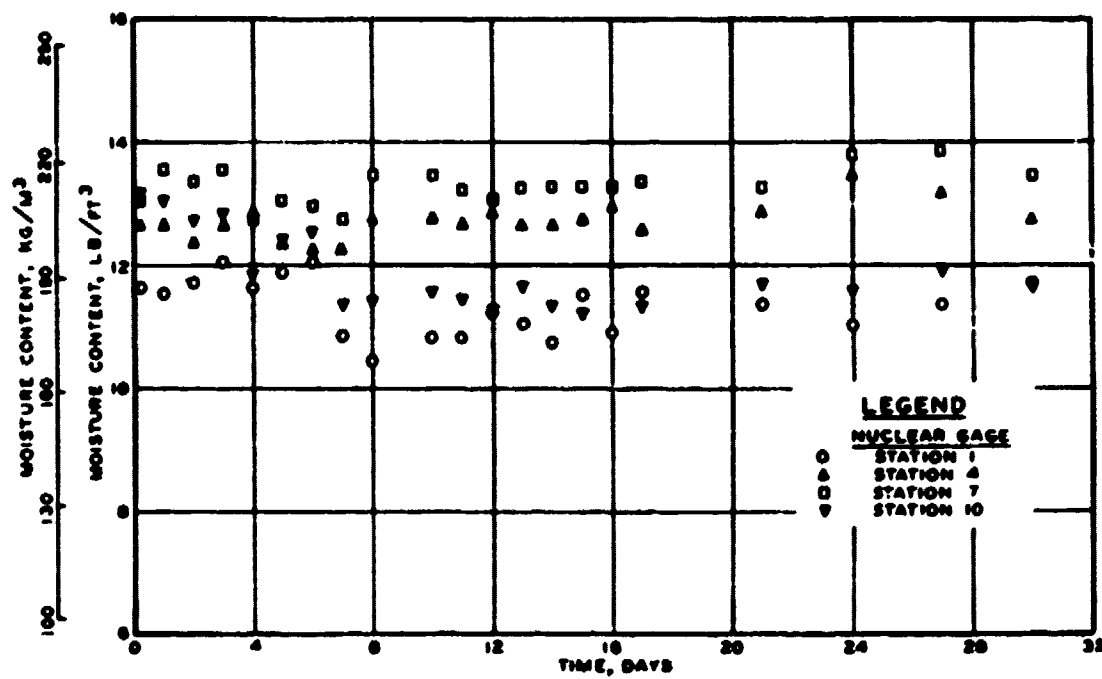


Fig. 11. Moisture content versus time

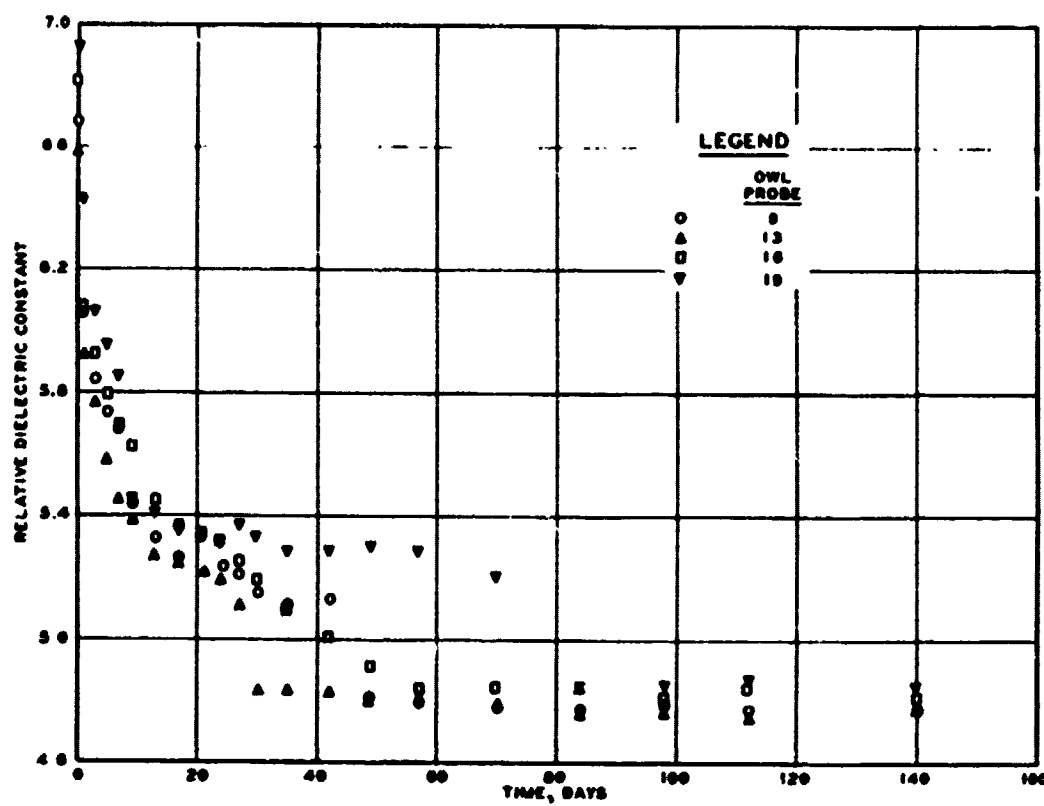


Fig. 12. Relative dielectric constant versus time

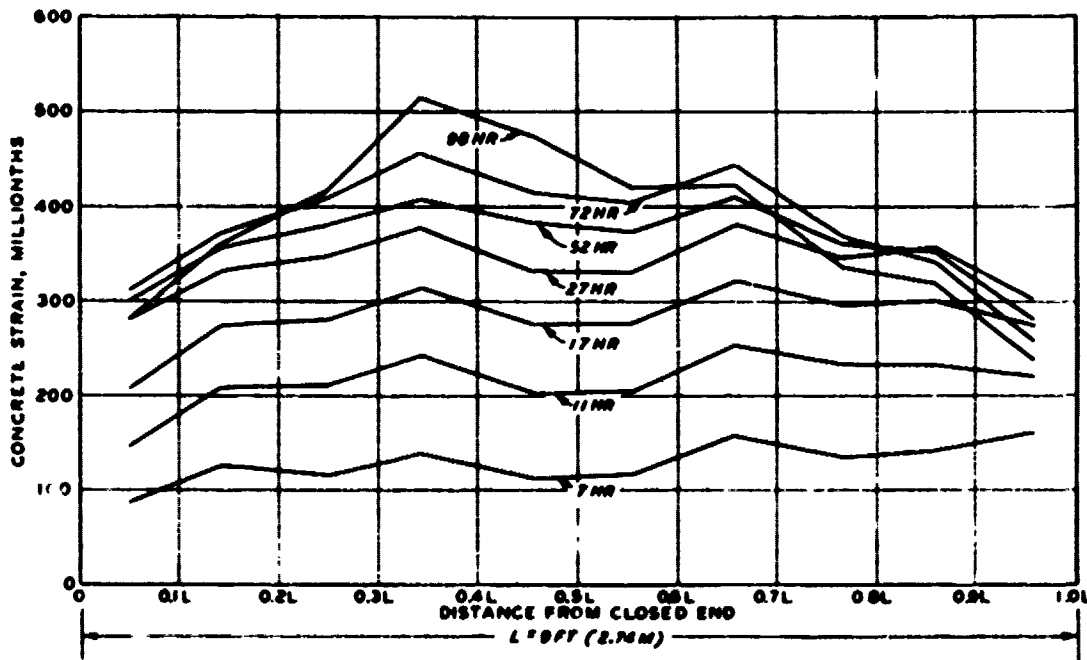


Fig. 13. Indicated strain distribution

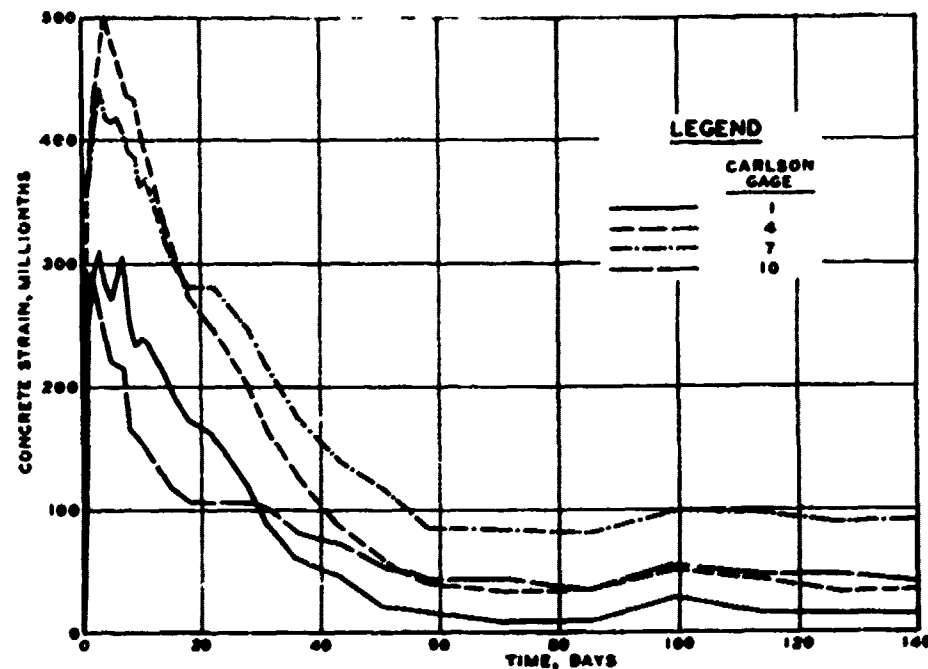


Fig. 14. Indicated strain versus time

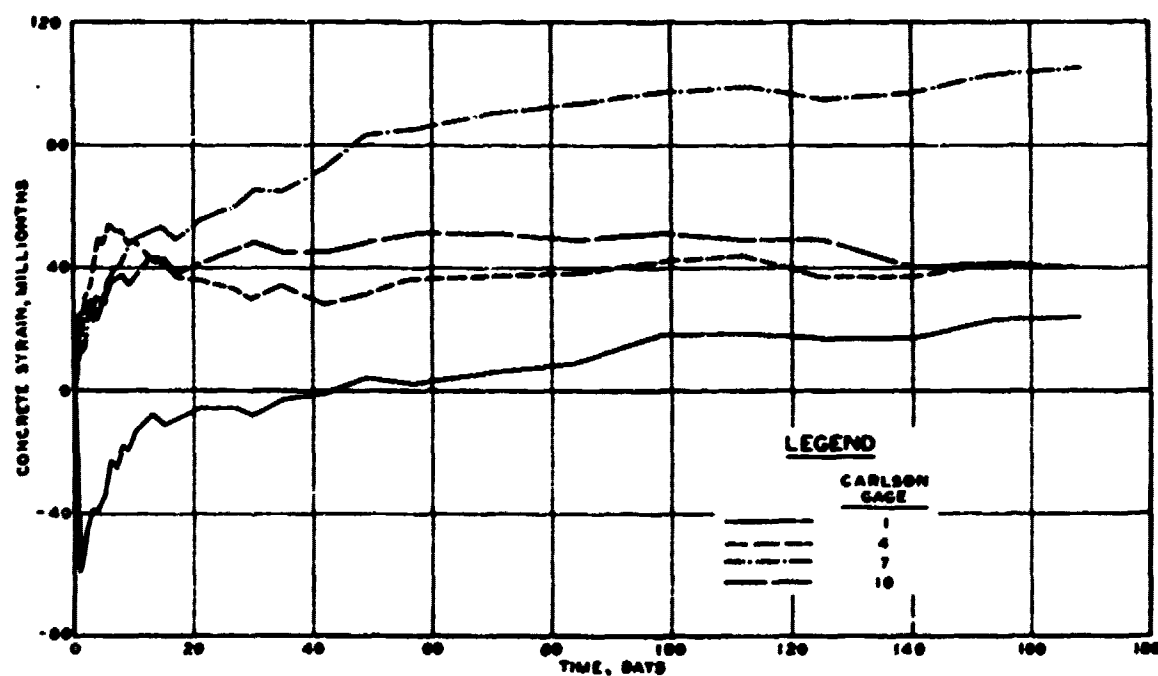


Fig. 15. Corrected strain versus time

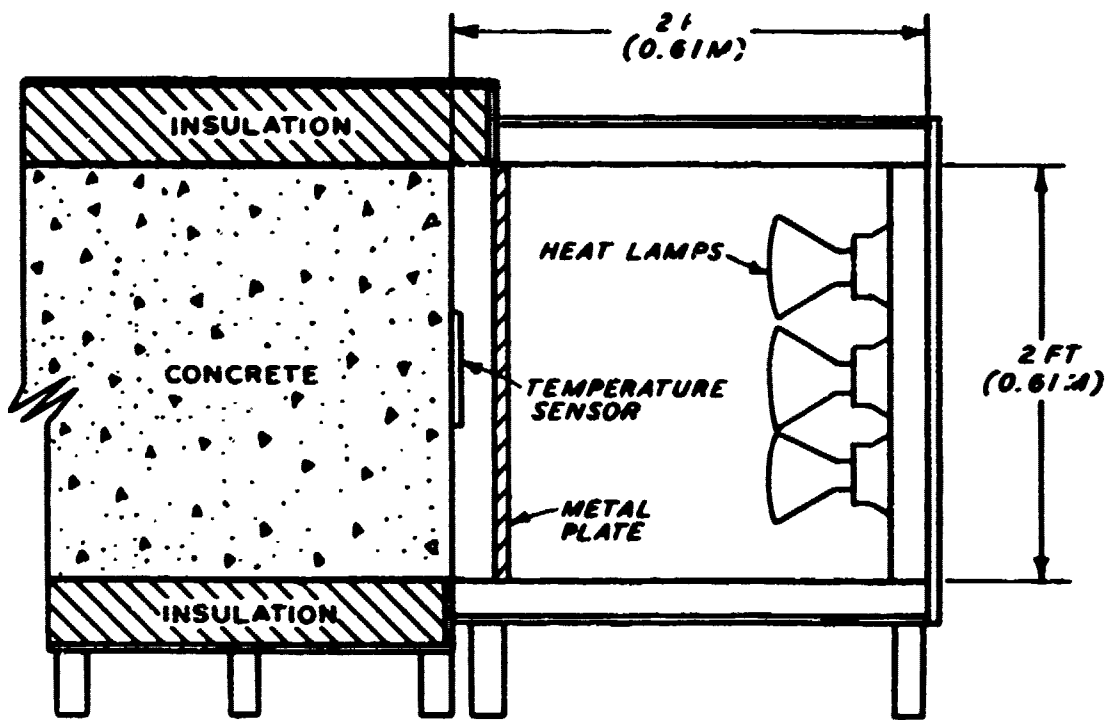


Fig. 16. Heating arrangement

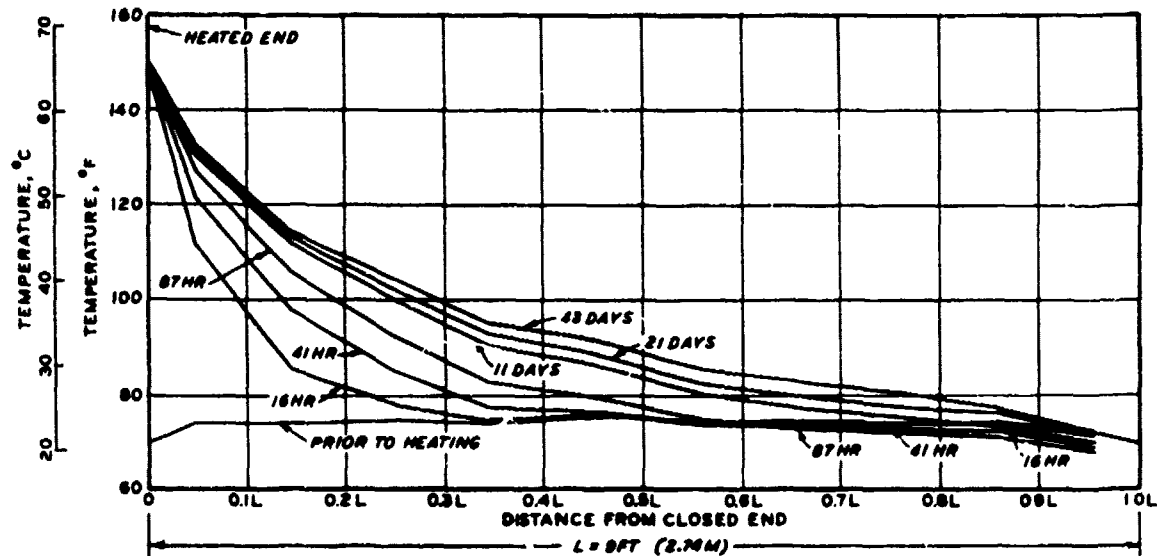


Fig. 17. Temperature variation along  $\ell$  of specimen after heating

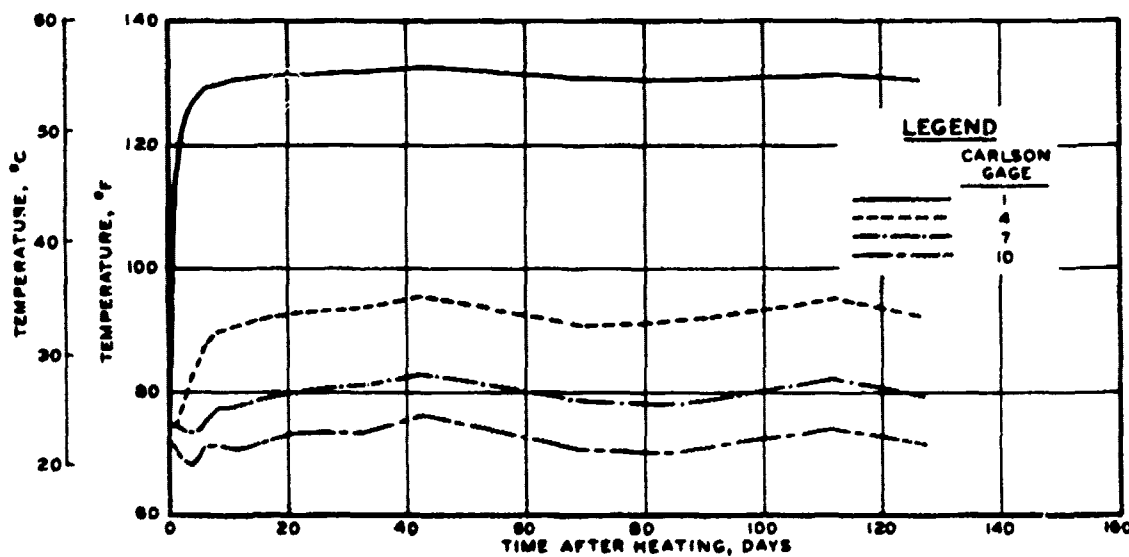


Fig. 18. Temperature versus time after heating

**THIS  
PAGE  
IS  
MISSING  
IN  
ORIGINAL  
DOCUMENT**

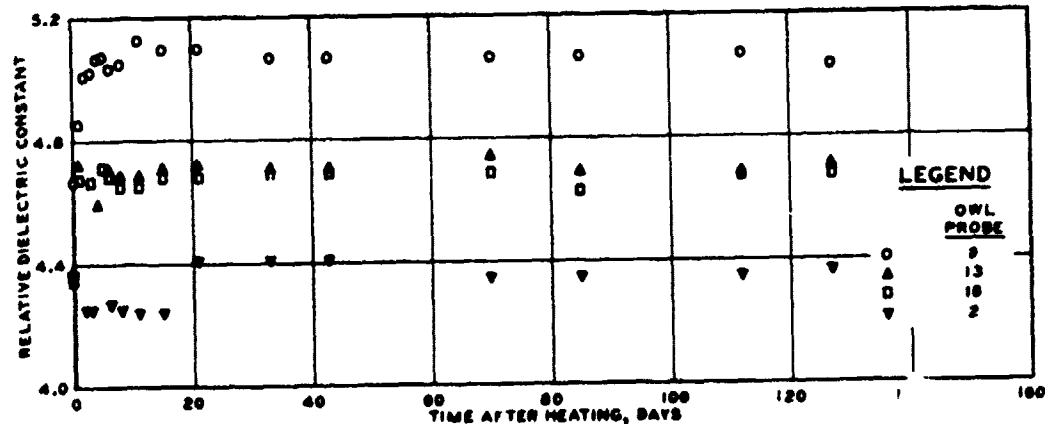


Fig. 21. Relative dielectric constant versus time after heating

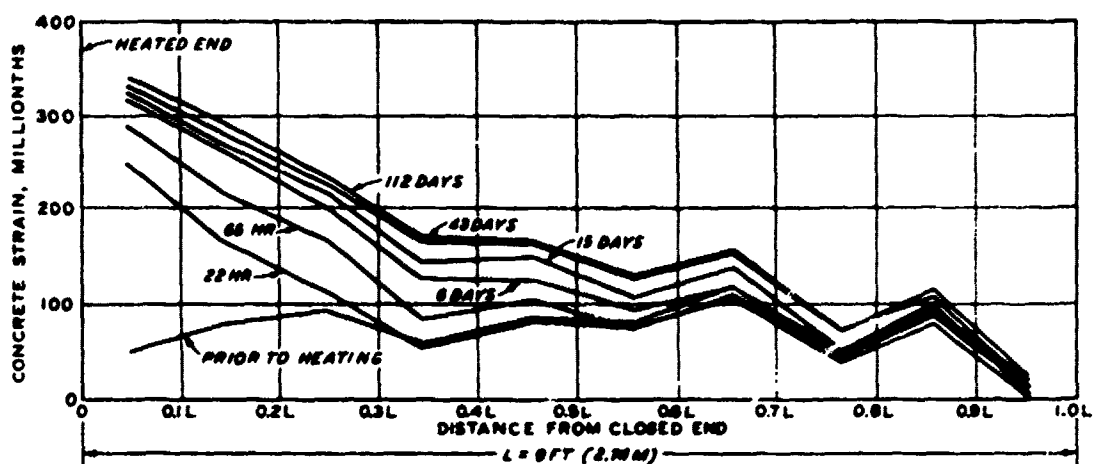


Fig. 22. Indicated strain distribution after heating

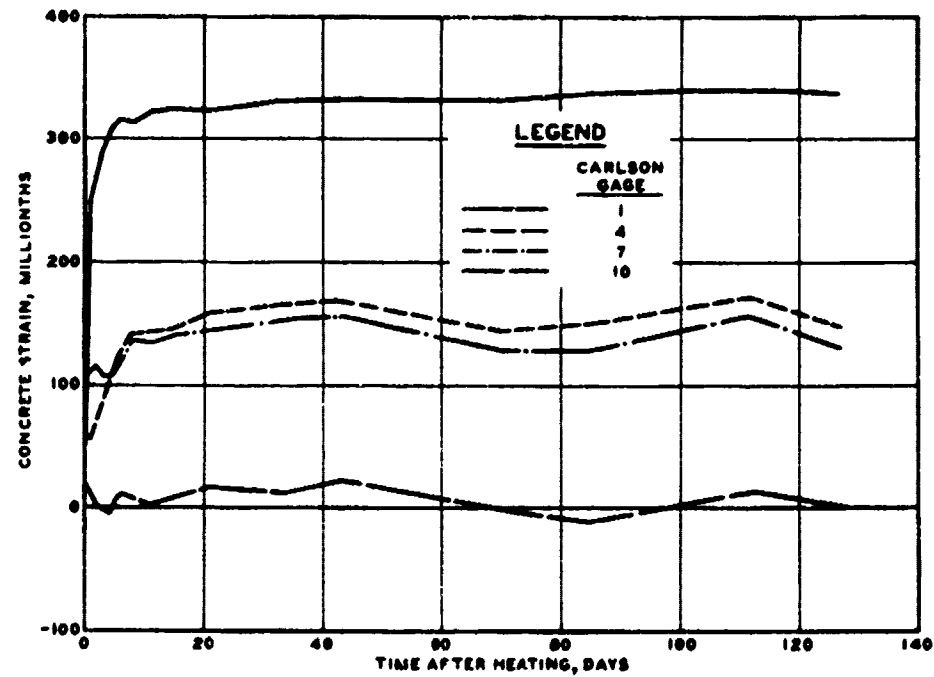


Fig. 23. Indicated strain versus time after heating

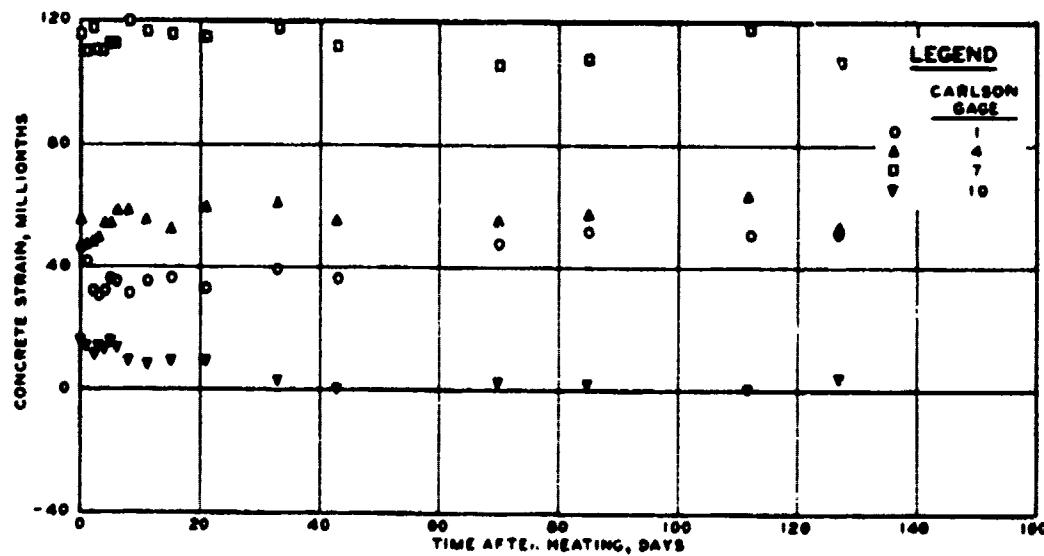


Fig. 24. Corrected strain versus time after heating